Standard ion transfer potential at the water|butyronitrile interface

J.S. Riva, V.C. Bassetto, H.H. Girault, A.J. Olaya

PII: S1572-6657(19)30049-9
DOI: https://doi.org/10.1016/j.jelechem.2019.01.041
Reference: JEAC 12871

To appear in: *Journal of Electroanalytical Chemistry*

Received date: 12 November 2018
Revised date: 15 January 2019
Accepted date: 15 January 2019

Please cite this article as: J.S. Riva, V.C. Bassetto, H.H. Girault, A.J. Olaya , Standard ion transfer potential at the water|butyronitrile interface. Jeac (2018), https://doi.org/10.1016/j.jelechem.2019.01.041

Standard ion transfer potential at the water|butyronitrile interface

J.S. Riva[a,b], V.C. Bassetto[a], H.H. Girault[a], A.J. Olaya*[,a]

[a]*Laboratoire d'Electrochimie Physique et Analytique, Ecole Polytechnique Fédérale de Lausanne, Rue de l'Industrie 17, CH-1951, Sion, Switzerland*

[b] *Consejo Nacional de Investigaciones Científicas y Técnicas, CONICET. Facultad de Matemática, Astronomía, Física y Computación, Universidad Nacional de Córdoba. Medina Allende s/n. Ciudad Universitaria, X5000HUA, Córdoba, Argentina.*

* Author to whom correspondence should be addressed: Dr. Astrid J. Olaya

E-mail: astrid.olaya@epfl.ch

Abstract

Butyronitrile is an organic solvent stable enough to be used in photochemical reactions at liquid/liquid interfaces. However, it provides a rather short polarisation window making the analysis of ion transfer across the water|butyronitrile interface challenging. Here, steady-state cyclic voltammetry, at microhole-supported micro-interfaces, was used to measure Gibbs energies of transfer. A linear relationship between the standard Gibbs energies of ion partition for the water|butyronitrile interface and the water|1,2-dichloroethane and water|nitrobencene interfaces was found, making easy to extrapolate the Gibbs energy of other ions from this empiric correlation.

1. Introduction

Electrochemistry at the interface between two immiscible electrolyte solutions (ITIES) allows for the study of ion transfer reactions across a liquid−liquid interface, and it has been used to analyse the transfer of antioxidants [1], surfactants [2] and ionisable drugs [3]. In addition, the ITIES provide an attractive platform to study challenging multi-electron transfer reactions in the field of energy such as hydrogen evolution [4], oxygen reduction [5] and water oxidation [6].

The most widely used solvents to study charge transfer across liquid|liquid interfaces are 1,2-dichloroethane (DCE) and nitrobenzene (NB), [7] however, they are highly unstable under

irradiation and/or in presence of strong oxidative agents. [8] In contrast, recently, butyronitrile (BCN) was found to be stable enough to be used for the water oxidation reaction at liquid/liquid interfaces [6]. Although the efficiency of the reaction was found to be strongly influenced by the chemical polarisation of the interface, the potential window of the water|BCN interface has not been assessed so far and therefore, the polarisation of the interface was not controlled. Indeed, the rather small potential window exhibited by the water|BCN interface makes the evaluation of standard transfer potentials ($\Delta_o^w f^0$) across this interface challenging when working at macro interfaces. However, the use of micro-ITIES considerably reduces the resistivity of the system, and therefore, supporting electrolytes in the aqueous or organic phase are no longer required. Thus, in this work we used the methodology reported by Olaya *et al.* [9] based on steady-state cyclic voltammetry at a microhole-supported micro-interface to separate the transfer of tetraphenylarsonium ($TPAs^+$) and tetraphenylborate (TPB^-) from the transfer of the supporting electrolytes. Wilke's [10] theoretical model was used to fit the voltammograms and therefore to estimate the $\Delta_o^w f^0$ of $TPAs^+$ and TPB^-, thus calibrating the water|BCN potential window. $\Delta_o^w f^0$ and $\Delta G_{tr}^{0,w\to o}$ of different ions across this interface were also estimated using this methodology.

2. Experimental

2.1. Chemicals

Butyronitrile (BCN, 99%) were purchased from Across, tetrapropylammonium chloride (TPACl > 98%), tetrapropylammonium bromide (TPABr > 98%) and tetraphenylarsonium chloride hydrate (TPAsCl, 99%) were purchased from ABCR, lithium chloride (LiCl ≥ 99%), bis(triphenylphosphoranylidene) ammonium chloride (BACl ≥ 97%), and tetrapropylammonium iodide (TPAI > 98%) were obtained from Sigma-Aldrich, and tetramethylammonium iodide (TMAI > 98%) and tetraethylammonium iodide (TEAI > 98%) were purchased from Fluorochem. Lithium tetrakis(pentafluorophenyl)borate (LiTB ≥ 98%) were purchased from Boulder Scientific Company.

Bis(triphenylphosphoranylidine)ammonium tetrakis(pentafluorophenyl)borate (BATB) and tetraphenylarsonium tetraphenylborate (TPAsTPB) were prepared by metathesis by using the

methods described previously [9]. All aqueous solutions were prepared in MilliQ water (18.2 MΩ·cm).

2.2. Ion transfer at the water|BCN interface

The cyclic voltammograms at the water|BCN macro interface were performed using the four-electrode cell described previously in reference 12. Thus, two reference electrodes (Ag/AgCl) polarise the interface and two platinum counter electrodes provide the current. The reference electrodes were connected to the aqueous and the organic phases by means of a Luggin capillary.

The micro-interface between water and BCN was supported on a microhole drilled in a 30 μm thick polyamide film (Kapton®, Dupont) purchased from Goodfellow (UK) by UV-photoablation using a Spirit 1040-4-SHG laser (Spectra Physics) with a μFAB Workstation (Newport). The diameter of the drilled microhole was 15 μm. The microhole was located in vertical position between the water and BCN using a Teflon cell previously described in reference 9 with two Ag/AgCl reference electrodes. For all the experiments, the voltammetric scan rate was 10 mV/s and the temperature was 20 °C. *IR* compensation for *IR* drop was not applied. In all the experiments the aqueous phase was introduced first and therefore, the interface was located on the organic side of the microhole [13].

The voltammetric experiments were carried out using potentiostat PGSTAT 302N, Metrohm Autolab (Herisau, Switzerland).

The composition of the electrochemical cells is shown in scheme 1.

3. Results

Figure 1 shows the potential windows recorded for the water|DCE and water|BCN macro-interfaces. The transfer of Li^+ and Cl^- limits the potential windows in the positive and negative side, respectively. In order to use the extra-thermodynamic TPAsTPB assumption to calibrate the potential window, $TPAs^+$ and TPB^- were added to the electrochemical cell, however, as observed in Figure 1, the potential window of the water|BCN macrointerface is only 200 mV wide, making it rather difficult to clearly separate the transfer of $TPAs^+$ and TPB^- from that of the ions composing the supporting electrolytes. The TPAsPB assumption considers that the standard Gibbs energy of partition of TPAsTPB can be split into two equal parts for

the cation and the anion because the radii of both ions are very similar ($\Delta G_{tr}^{0,w\rightarrow o}(TPAs^{+}) = \Delta G_{tr}^{0,w\rightarrow o}(TPB^{-})$), therefore, the zero of the $\Delta_o^w f_{1/2}$ scale is located in the middle of the half-wave potentials of both ions [14].

		Aqueous Phase	Organic Phase (BTN or DCE)				
Ag |	AgCl |	LiCl 10mM	BATB 10mM	BACl 1mM LiCl 10mM	| AgCl |	Ag	**I**
Ag |	AgCl |	LiCl 10mM	BATB 10mM TPAsTPB 0.5mM	BACl 1mM LiCl 10mM	| AgCl |	Ag	**II**
Ag |	AgCl |	water	BATB 0.1mM	BACl 1mM LiCl 10mM	| AgCl |	Ag	**III**
Ag |	AgCl |	water	BATB 0.1mM TPAsTPB 0.1mM	BACl 1mM LiCl 10mM	| AgCl |	Ag	**IV**
Ag |	AgCl |	$TPA^{+}Y^{-}$ 0.5mM	BATB 0.1mM $X^{+}I^{-}$ 0.5mM	BACl 1mM LiCl 10mM	| AgCl |	Ag	**V**
Ag |	AgCl |	$X^{+}I^{-}$ 0.5mM	BATB 0.1mM $TPA^{+}Y^{-}$ 0.5mM	BACl 1mM LiCl 10mM	| AgCl |	Ag	**VI**

Scheme 1. Configuration of the cells for the ion-transfer voltammetric studies at the water|BCN interface. X correspond to the cations: TPA^{+}, TEA^{+}, TMA^{+}. Y^{-} corresponds to the anions: I^{-}, Br^{-} and Cl^{-}. Cells I and II were studied in macro-ITIES, and cells III, IV, V and VI were studied in micro-ITIES.

Considering that the use of micro-ITIES largely decreases the *IR* drop and therefore the presence of supporting electrolytes is no longer necessary, we have used the methodology described by Olaya *et al.* based on steady-state cyclic voltammetry under unsupported conditions [9], and Wilke's *et al.* theoretical model [10,11], to determine the transfer potential of $TPAs^{+}$ and TPB^{-} among other ions at the water|BCN micro-interface (Fig. 2).

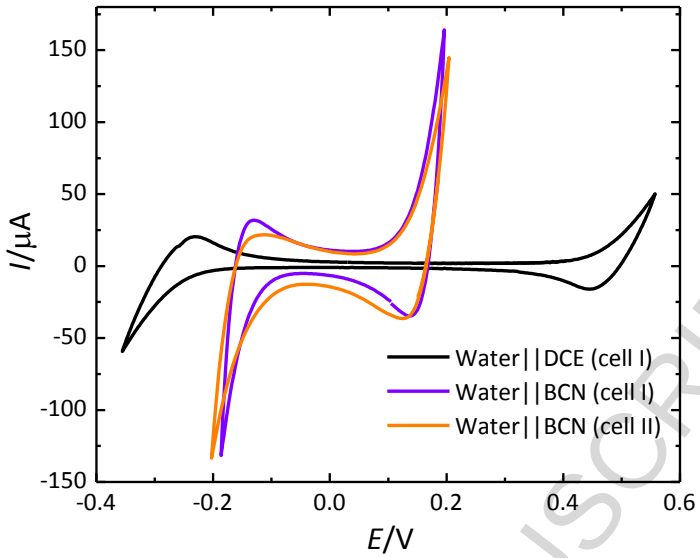

Fig. 1. Comparison of the potential windows at macro-interfaces using DCE (black) or BCN (violet) as organic solvent (cell I). Cyclic voltammogram of transfer of TPAsTPB in a Water/BCN macro-interface (orange, cell II). Scan rate: 25 mV·s^{-1}.

The model described by Wilke *et al.* [11] for unsupported systems (without supporting electrolyte in the aqueous phase) considers that the voltage available for the polarisation of the micro-interface is reduced by the potential drop in the aqueous phase. The $D_0^w f_{1/2}$ calculated with $I = I_{lim}/2$ is shifted from the usual half-wave potential by

$$D_0^w f'_{1/2,A} - D_0^w f_{1/2,A} = \frac{RT}{z_A F} \ln\left[2^{-z_A/z_B}\left(1-\frac{z_A}{z_B}\right)\right] \quad (1)$$

where z_A is the cation charge number, z_B is the anion charge number, R is the molar gas constant, T is the temperature and F is the Faraday constant. As in all experiments the condition $z_A = -z_B$ is fulfilled, I_{lim} and $D_0^w f$ can be expressed as [11]:

$$I_{\text{lim}} = 8 z_A F D_{A,w} c_A \quad (2)$$

where $D_{A,w}$ and c_A are the diffusion coefficient and the concentration of ion *A* respectively. And the total potential difference ($\Delta_o^w f$) as a function of the cell current, can be expressed as:

$$\Delta_o^w f_A = \Delta_o^w f_{1/2,A} + \frac{RT}{z_A F} \ln\left[2\left(\frac{I}{I_{\lim} - I} \right)\left(\frac{I_{\lim}}{I_{\lim} - I} \right) \right]$$

(3)

Therefore, the current can be written as function of the potential difference as,

$$I = I_{\lim}\left[1 + \exp\left[\frac{z_A F}{RT}\left(\Delta_o^w f - \Delta_o^w f_{1/2,A} \right) \right] - \sqrt{\left[1 + \exp\left[\frac{z_A F}{RT}\left(\Delta_o^w f - \Delta_o^w f_{1/2,A} \right) \right] \right]^2 - 1} \right] \quad (4)$$

And, the relationship between $\Delta_o^w f_{1/2}$ and the standard transfer potentials $\Delta_o^w f$ in a micro-interface can be expressed as [10]:

$$\Delta_o^w f_{1/2} = \Delta_o^w f^0 + \frac{RT}{zF} \ln\left(\frac{D_w}{D_o} \right) + \frac{RT}{zF} \ln\left(\frac{\gamma_w}{\gamma_o} \right) + \frac{RT}{zF} \ln\left(\frac{4d}{\pi r} + 1 \right) \quad (5)$$

Were D_w, D_o, γ_w and γ_0 are the respective diffusion coefficients and activity coefficients in aqueous and organic phases, *d* is the depth of the microhole (being equal to the film thickness (30μm) and *r* the radius (15μm). The last term represents the correction due to the asymmetry of the mass transport, which is radial in the organic phase and linear in water inside the channel. Under the present conditions, this is only 21mV/*z*. The ratio D_w/D_o was estimated by using Walden's rule $\eta_w D_w = \eta_o D_o$, with η being the viscosity. The viscosities of water and BCN are 0.00091 P·s and 0.0000553 P·s (at 25 °C) [15], respectively, therefore, D_w/D_o=0.0607 and the second term is equal to –71.9 mV/*z*. The activity coefficients have been calculated by using the extended Debye–Hückel law [10],

$$\log_{10} \gamma_i = \frac{-A z_i^2 \mu_i^{1/2}}{1 + B a_i \mu_i^{1/2}} \quad (6)$$

where μ_i is the ionic strength and a_i is the diameter of the hydrated ion *i*, which for the ions studied in this work can be assumed as 0.3 nm in the aqueous phase and 0.6 nm in the organic phase [15]. The constants *A* and *B* were estimated by using Eqs. (7) and (8),

$$A\left(\frac{\mathrm{L}\cdot\mathrm{K}^3}{\mathrm{mol}}\right)^{1/2}=\frac{1.8245\cdot10^6}{(\varepsilon_r T)^{3/2}} \tag{7}$$

$$B\left(\frac{\mathrm{L}\cdot\mathrm{K}}{\mathrm{mol}\cdot\mathrm{nm}^2}\right)^{1/2}=\frac{502.904}{(\varepsilon_r T)^{1/2}} \tag{8}$$

were ε_r is the relative electrical permittivity and T is the temperature on the Kelvin scale. Thus, the obtained values were A=0.5 (3.97) $\mathrm{L}^{1/2}\cdot\mathrm{mol}^{-1/2}$ and B=3.28 (6.40) $\mathrm{L}^{1/2}\cdot\mathrm{mol}^{-1/2}\cdot\mathrm{nm}^{-1}$ (at 25 ºC) for water (butyronitrile), and the third correction term is equal to 19.04 mV/z.

$$\Delta_o^w f_{1/2,A}=\Delta_o^w f_A^0-\frac{31.86\mathrm{mV}}{z_A} \tag{9}$$

Finally, the standard Gibbs energy of the ion transfer ($\Delta G_{\mathrm{tr}}^{0,\mathrm{w}\to\mathrm{o}}$) is:

$$\Delta G_{\mathrm{tr},A}^{0',\mathrm{o}\to\mathrm{w}}=-z_A F\Delta_o^w f_{1/2,A} \tag{10}$$

Figure 2, 3a and 3b records the experimental steady-state voltammograms obtained for the cells described in Scheme 1 (very low concentration of BATB in the organic phase, and in absence of supporting electrolyte in the aqueous phase). As expected, the use of unsupported conditions allowed for the clear observation of the transfer of TPAs^+ and TPB^-, therefore, the $\Delta_o^w\phi_{1/2}$ scale of the water|BCN interface was successfully calibrated. The term $\frac{RT}{z_A F}$, which was replaced by the experimental parameter S, and the experimental parameters I_{lim} and $\Delta_o^w\phi_{1/2}$, were estimated by fitting the data recorded in Figures 2 and 3 with equation 4 (Table 1). The S values obtained from the fitting are lower than the expected 38.9 V^{-1}, especially for cells II and III were no electrolytes were added to the aqueous phase making the *IR* drop more significant. However, when comparing the $\Delta_o^w\phi_{1/2}$ obtained when forcing S to the theoretical value, with the $\Delta_o^w\phi_{1/2}$ obtained with the S values obtained by iteration, the difference is only 20 mV.

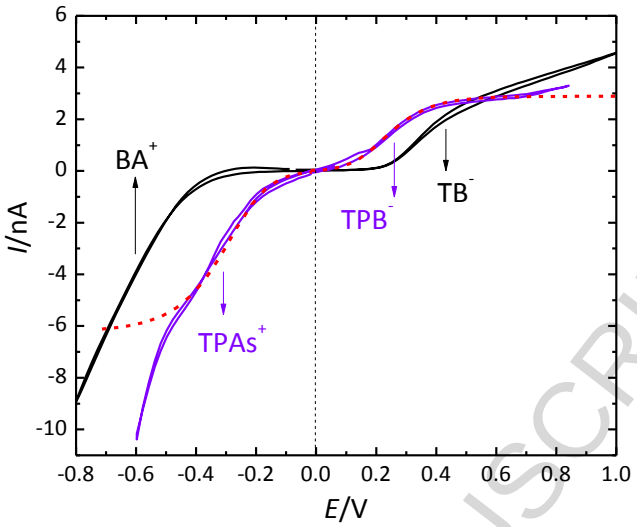

Fig. 2. Calibration of the potential window at the water|BCN microinterface under unsupported conditions using the TPAsTB assumption. Cyclic voltammograms obtained with cell III (black) and cell IV (violet). Scan rate: 10 $mV \cdot s^{-1}$. Dashed line: non-linear curve fitting with equation 4.

In addition, TMA^+, TEA^+, TPA^+, Cl^-, Br^- and I^-, were studied at the water|BCN micro-interface, in order to determine if they follow the same trend as at the water|DCE and water|NB interfaces. The steady-state voltammograms obtained in absence of supporting electrolyte in the aqueous phase (cells V and VI in Scheme 1) are shown in Figure 3a and 3b for anions and cations, respectively. The solid lines represent the experimental data, whereas the dashed lines represent the fitting made using equation 4. Ion transfer parameters were calculated and summarized in Table 1.

Figure 4 shows the relationship between the $\Delta G_{tr}^{0,w\rightarrow o}$ obtained at the water|BCN interface and the $\Delta G_{tr}^{0,w\rightarrow o}$ reported for the water|DCE [17] and water|NB [18,19] interfaces. In both cases, linear relationships were found, which is in good agreement with previous works for other solvents [15]. The slopes of the correlation curves are 0.718 and 0.762 when comparing with DCE and NB, respectively, and the intercepts are 6.18 (BCN *vs* DCE) and 11.74 (BCN vs NB) indicating that the $\Delta G_{tr}^{0,w\rightarrow BCN}$ are smaller than those reported for the transfer to NB and DCE.

These values also correlate well with those found by other authors for similar comparisons suggesting that the $\Delta G_{\mathrm{tr}}^{0,\mathrm{w}\to\mathrm{o}}$ determined at the water|DCE and water|NB interfaces, could be used to estimate $\Delta G_{\mathrm{tr}}^{0,\mathrm{w}\to\mathrm{o}}$ at the water|BCN interface by using these empirical relationships.

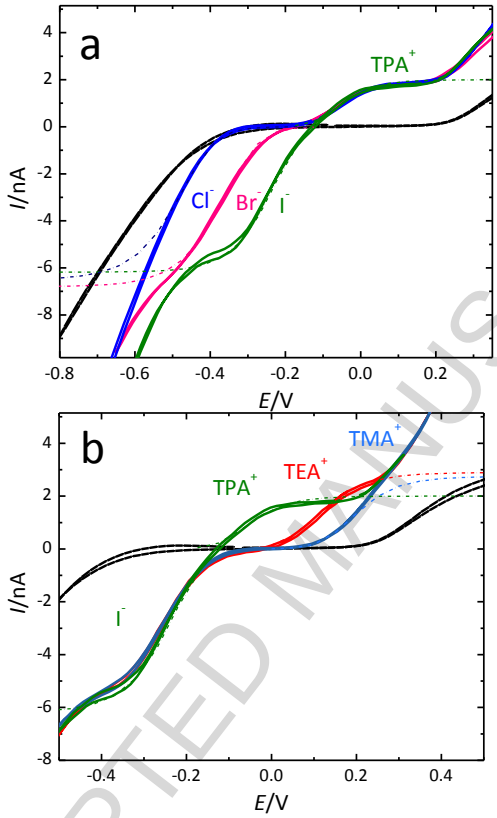

Fig. 3. Voltammograms of different (a) anions, cell V, and (b) cations, cell VI, in water|BCN microinterfaces. Scan rate: 10 mV·s^{-1}. Dashed line: non-linear curve fitting with equation 4.

Table 1. Experimental current, I_{lim}, half wave potentials, $\Delta_o^w\phi_{1/2}$, standard transfer potentials $\Delta_o^w\phi^0$, standard Gibbs energies of partition $\Delta G_{tr}^{0,w\to o}$ and S parameter for ion transfer at the water|BCN interface. I_{lim}, $\Delta_o^w\phi_{1/2}$ and S were estimated by non-linear curve fitting of the experimental data with equation 4. Standard transfer potentials were corrected by considering eq. 9, and standard Gibbs energies were calculated from eq. 10.

	I_{lim}/nA	$\Delta_o^w\phi_{1/2}$/V	$\Delta_o^w\phi^0$/V	$\Delta G_{tr}^{0,w\to o}$/kJ · mol^{-1}	S/V^{-1}
$TPAs^+$	–0.64	–0.210	–0.178	–17.18	–19.00
TPB^-	2.88	0.210	0.178	–17.18	22.90
Cl^-	–6.5	–0.394	–0.426	41.10	26.68
Br^-	–6.80	–0.298	–0.330	31.83	27.00
I^-	–6.42	–0.208	–0.240	23.15	30.29
TPA^+	2.03	–0.102	–0.070	–6.77	–35.89
TEA^+	2.89	0.073	0.105	10.12	–30.00
TMA^+	2.74	0.159	0.191	18.42	–32.34

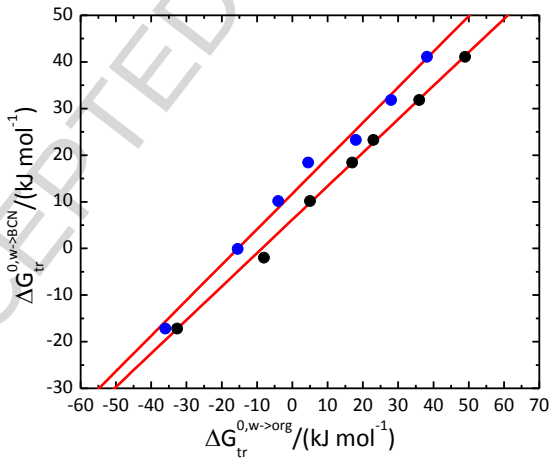

Fig. 4. Correlation of standard Gibbs transfer energies from water to BCN and the values reported at water|DCE interface (black points) [16] and water|NB (blue points) [17,18] interfaces.

4. Conclusion

The water/BCN interface was successfully calibrated by using the methodology reported by Olaya *et al*. [9], based on steady-state cyclic voltammetry at a microhole-supported micro-interface and Wilke's *et al.* [10] theoretical model. The $\Delta_o^w\phi^0$ and $\Delta G_{tr}^{0,w\to o}$of different ions across this interface were also estimated using this methodology.

A linear relationship was found between the values of $\Delta G_{tr}^{0,w\to o}$ in water| BCN interface and the values of $\Delta G_{tr}^{0,w\to o}$ in other organic solvents, as DCE and NB, therefore, the $\Delta G_{tr}^{0,w\to o}$ determined at the water|DCE and water|NB interfaces, could be used to estimate $\Delta G_{tr}^{0,w\to o}$at the water|BCN interface by using these empirical relationships. The slopes and the intercepts of the correlation curves are 0.718 and 6.18, respectively, when comparing with DCE, and 0.762 and 11.74, respectively, when comparing with NB, indicating that the $\Delta G_{tr}^{0,w\to BCN}$ are smaller than those reported for the transfer to NB and DCE.

5. References

[1] J.A. Ribeiro, S. Benfeito, F. Cagide, J. Teixeira, P.J. Oliveira, F. Borges, A.F. Silva, C.M. Pereira, Electrochemical Behaviour of a Novel Mitochondria-targeted Antioxidant at an ITIES: an Alternative Approach to Study Lipophilicity, Anal. Chem., 90 (13) (2018) 7989-7996.

[2] B.N. Viada, A.V. Juarez, E.M. Pachon Gomez, M.A. Fernandez, L.M. Yudi, Determination of the critical micellar concentration of perfluorinated surfactants by cyclic voltammetry at liquid/liquid interfaces, Electrochim. Acta, 263 (2018) 499-507.

[3] J.A. Ribeiro, F. Silva, C.M. Pereira, Electrochemical study of the anticancer drug daunorubicin at a water/oil interface: drug lipophilicity and quantification, Anal. Chem. 85 (2013) 1582-1590.

[4] L. Rivier, T.J. Stockmann, M.A. Méndez, M.D. Scanlon, P. Peljo, M. Opallo, H.H. Girault. Decamethylruthenocene Hydride and Hydrogen Formation at Liquid|Liquid Interfaces, J. Phys. Chem. C, 119 (2015) 25761−25769.

[5] M.A. Kamyabi, F. Soleymani-Bonoti, R. Bikas, H. Hosseini-Monfared, Oxygen reduction catalyzed by a Carbohydrazone based compound at liquid/liquid interfaces, J.

Electroanal. Chem., 794 (2017) 235–243.

[6] S. Rastgar, M. Pilarski, G. Wittstock, Polarized liquid-liquid interface meets visible-light-driven catalytic water oxidation, Chem. Commun., 52 (2016) 11382-11385.

[7] V. Sladkov, V. Guillou, S. Peulon, M. L'Her, Voltammetry of tetraalkylammonium picrates at water|nitrobenzene and water|dichloroethane microinterfaces; influence of partition phenomena, J. Electroanal. Chem., 573 (2004) 129–138.

[8] A.J. Olaya, P.F. Brevet, E.A. Smirnov, H.H. Girault, Ultrafast Population Dynamics of Surface-Active Dyes during Electrochemically Controlled Ion Transfer across a Liquid|Liquid Interface, J. Phys. Chem. C, 118 (43) (2014) 25027–25031.

[9] A.J. Olaya, M.A. Méndez, F. Cortés-Salazar, H.H. Girault, Voltammetric determination of extreme standard Gibbs ion transfer energy, J. Electroanal. Chem., 644 (2010) 60-66.

[10] S. Wilke, T. Zerihun, Standard Gibbs energies of ion transfer across the water | 2-nitrophenyl octyl ether interface, J. Electroanal. Chem., 515 (2001) 52–60.

[11] S. Wilke, Current–potential curves for liquid|liquid microinterfaces with no added supporting electrolyte in the water phase, J. Electroanal. Chem., 504 (2001) 184–194

[12] M.A. Méndez, R. Partovi-Nia, I. Hatay, B. Su, P. Ge, A. Olaya, N. Younan, M. Hojeij, H.H. Girault, Molecular electrocatalysis at soft interfaces, Phys. Chem. Chem. Phys., 12 (2010) 15163–15171.

[13] S. Peulon, V. Guillou, M. L'Her, Liquid liquid microinterface. Localization of the phase boundary by voltammetry and chronoamperometry; influence of the microchannel dimensions on diffusion, J. Electroanal. Chem., 514 (2001) 94-102.

[14] A.J. Olaya, P. Ge, H.H. Girault, Ion transfer across the water|trifluorotoluene interface, Electrochem. Commun., 19 (2012) 101–104.

[15] S. Creager, Solvents and Supporting Electrolytes, in: Zoski, C.G. (ed.) Handbook of Electrochemistry, Elsevier, Amsterdam (2007) 57-72.

[16] M.H. Abraham, A.F. Danil de Namor, Solubility of electrolytes in 1,2-dichloroethane and 1,1-dichloroethane, and derived free energies of transfer, J. Chem. Soc. Faraday Trans. 1 (72) (1976) 955-962.

[17] A.F. Danil de Namor, T. Hill, Elizabeth Sigstad, Free energies of transfer of 1:1 electrolytes from water to nitrobenzene. Partition of ions in the water + nitrobenzene system, J. Chem. Soc. Faraday Trans. 1 (79) (1983) 2713-2722.

[18] B. Hundhammer, S. Wilke, Investigation of ion transfer across the membrane stabilized interface of two immiscible electrolyte solutions, J. Electroanal. Chem., 266 (1989) 133-141.

Highlights

- Butyronitrile is a stable solvent under illuminated and/or in the presence of strong oxidants.
- The water/BCN interface is calibrated by using steady-state cyclic voltammetry at a microhole-supported micro-interface.
- There is a linear relationship between the values of $\Delta G_{\mathrm{tr}}^{0,\mathrm{w}\to\mathrm{o}}$ in water| BCN interface and the values of $\Delta G_{\mathrm{tr}}^{0,\mathrm{w}\to\mathrm{o}}$ in other organic solvents, as DCE and NB.